1. THE INFLUENCE OF SEGMENT INTERFACE CHARACTERISTICS ON SEISMIC PERFORMANCE OF POST-TENSIONED PRECAST SEGMENTAL BRIDGE PIERS

Cancan Yang, Dept. of Civil, Structural, and Environmental Engineering, Uni. at Buffalo, Buffalo, NY
Pinar Okumus, PhD, Dept. of Civil, Structural, and Environmental Engineering, Uni. at Buffalo, Buffalo, NY

ABSTRACT

The *seismic performance of precast concrete segmental piers post-tensioned with unbonded strands was through analytical modeling developed based on test results. Similar low-damage precast concrete segmental bridge columns have been proposed for seismic regions for their accelerated bridge construction benefits. Unlike these systems, piers presented in this paper allowed shear-slip to dissipate energy through friction. Segments are prefabricated without shear keys to allow shear-slip. Unbonded post-tensioning provided self-centering capabilities.*

Previous quasi-static cyclic testing showed that segment interface friction properties determine the amount of energy dissipation. The impact of surface characteristics on the seismic performance was investigated by developing an analytical model. The analytical model predicts the overall load-displacement behavior of piers under lateral loading by superposing self-centering and shear-slip responses. Shear-slip under lateral loading was measured and used to characterize the interface frictional properties used in analytical modeling.

A parametric analysis was performed using the analytical model to investigate the influence of friction properties of commonly used interface materials on seismic performance. The results show that energy dissipation is strongly associated with friction and shear-slip. Reduction in friction coefficient increases energy dissipation, decreases stiffness, and increases residual displacements.

Keywords: Analytical model, Shear-slip, Rocking, Precast Substructure, Post-Tensioning, Segmental Bridge

INTRODUCTION

Precast concrete bridge construction can shorten construction time, improve quality, improve construction safety and reduce the environmental impact by moving critical construction activities to prefabrication plants. Another advantage of precast concrete in seismic zones is its ability to accommodate self-centering systems through non-emulative connections. Non-emulative precast concrete systems, accompanied by un-bonded post-tensioning, can efficiently control seismic damage and limit residual displacements[1-3]. Nonlinear-elasticity is provided through joint opening, preventing the formation of plastic hinges[4]. Energy dissipation can be achieved in two ways. One method is to dissipate energy through yielding by adding internal yielding steel bars[5-7], or replaceable external yielding dampers[8-10]. The other means for adding energy dissipation is to introduce shear-slip through friction. Friction dampers, activated by beam-to-column joint opening, have been shown to provide supplemental energy dissipation[11]. Similarly, pier segment joints intentionally designed to slide can provide energy dissipation through friction with small damage[12,13]. Energy dissipation through friction is the focus of this paper.

Although friction is an efficient method to dissipate energy, response can highly depend on the friction properties of the sliding surfaces. Friction devices, such like seismic isolation bearings and friction dampers, often use polytetrafluoroethylene (PTFE) type composite materials against polished stainless steel or bronze against stainless steel. Numerous studies have shown the dependency of the friction coefficient on the apparent pressure, velocity of sliding, and temperature[14,15]. For example, friction coefficient for unlubricated PTFE in contact with polished stainless steel was measured in the range of 0.05 to 0.008 for apparent pressure varying from 0.9 to 6.7 ksi (6 to 46 MPa) at low velocity of sliding[16-19]. The sliding friction coefficient increases with increasing velocity of sliding. As for leaded bronze against stainless and alloy cast steel, Morgen and Kumara[20] reported the average static friction coefficient to be 0.209 and 0.248, the average kinetic friction coefficient to be 0.161 to 0.190 for normal force of 13 to 65 kips (58 to 289 kN) respectively. Furthermore, friction properties, especially the coefficient of friction, may also change over the design life due to aging, creep, corrosion, contamination, fatigue, and cumulative movement[14,21].

The precast concrete segmental pier presented in this paper allowed shear-slip to dissipate energy through friction. Segments were prefabricated without shear keys to allow shear-slip. The sliding interface was created by applying a layer of silicone at interfaces between precast pier segments. Quasi-static testing was performed on a specimen with fresh silicone surfaces, and on the same specimen with degraded silicone or dry concrete surfaces. Degradation of silicone in this specimen was caused mainly by accumulating movement between segments from previous testing. In general, degradation of silicone may also be caused by aging and environmental changes such as temperature and drying, in addition to movement under service and seismic loads. The test results for the two different sliding interfaces were compared to understand the effects of shear-slip on the response.

A mechanics based analytical model is proposed. The experimental results were used to characterize the shear-slip frictional response to be used in the analytical model. A

parametric study, where friction property was the variable, was performed to demonstrate the influence of segment interface properties on the seismic performance.

RESEARCH SIGNIFICANCE

Traditional segmental precast concrete columns have connections that emulate cast-in-place concrete behavior by preventing joint opening and shear-slip. Although segmental columns with traditional and emulative connections have performed well under seismic loading, they undergo irreparable damage to dissipate energy. The concept presented in this paper aims at minimizing seismic damage in bridge columns so that bridges can remain operational after a seismic event. Intentionally allowing shear-slip between segments can be a good resource of energy dissipation, without creating significant damage. This paper evaluates the sensitivity of shear-slip response to variation in segmental interface characteristics through experimental and analytical studies.

EXPERIMENTAL INVESTIGATION

The tests were conducted at a 1 to 2.4 length-scale bridge pier model. The overall experimental set-up is shown in Fig. 1 (a). Pier specimen design followed the design by Sideris et al.[12], but was modified according to the constraints of the test set-up used in this study. The specimen consists of a precast concrete foundation element, a precast concrete cap beam, and five precast concrete hollow column segments. All of the precast elements were made of conventional 5 ksi (34.5 MPa) compressive design strength concrete. They were connected to each other with eight unbonded post-tension strands. Post-tensioning strands were 7 wire, 0.6 in. (15.2 mm) diameter, low relaxation strands, with 270 ksi (1862 MPa) ultimate strength.

The post-tensioning strands were fitted into ungrouted flexible polyvinyl chloride (PVC) corrugated ducts with an interior diameter of at least 0.9 in. to accommodate the movement of unbonded strands within the ducts. The segments were prefabricated manually and abundantly without shear keys to allow shear-slip. A layer of silicone was applied at segment interfaces to reduce the friction coefficient between segments, as seen in Fig. 1 (b). Pressure between segments due to weight distributed silicone over the segment surface.

(a) (b)

Fig. 1 (a) Experimental setup and (b) application of fresh silicone at segmental interface

Two quasi-static cyclic tests were conducted on the specimen. The first quasi-static test was performed on the specimen when it had fresh silicone between segments, allowing shear-slip. The second quasi-static cyclic test was performed on the same specimen, which was previously tested but not damaged, and which had deteriorated silicone between segments. The second quasi-static cyclic test was preceded by the first quasi-static test and several dynamic tests.

The comparison of hysteretic loop of pier specimen with fresh silicone and degraded silicone is shown in Fig. 2. Pier with fresh silicone interfaces had a fatter hysteretic load-displacement curve with energy dissipation associated with shear-slip. Shear-slip also increased residual displacements and caused misalignment of some segments upon removal of load. Specimens with degraded silicone interfaces exhibited rocking over the precast foundation, resulting in reduced energy dissipation but better self-centering. The lateral strength was smaller when shear-slip was allowed compared to one for the specimen with no shear-slip.

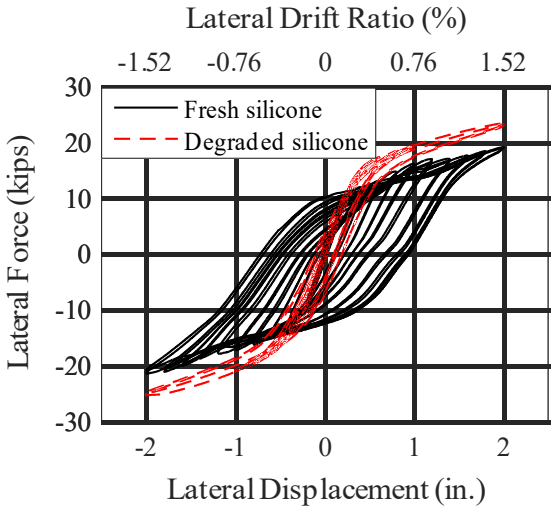

Fig. 2 Hysteretic responses of specimen with fresh and degraded silicone between segments

The stiffness of pier with fresh silicone was smaller than degraded silicone, which can reduce the maximum acceleration response and the associated seismic force. This softening effect may cause an increase in displacements, which can be offset by the increasing energy dissipation provided by shear-slip. Designers can proportion columns to find a balance between energy dissipation and residual displacements, according to project needs and performance requirements.

The impact hammer testing conducted before the first and second quasi-static tests indicated similar dynamic properties (i.e., fundamental frequency and viscous damping). This confirmed that there was virtually no damage due to the first test and that the difference between the hysteretic responses from the two tests is caused by the difference in segment interfaces. Silicone condition and properties may change over the design life. The resulting change in seismic behavior should be considered in design if silicone used for segment interfaces to facilitate shear-slip.

CHARACTERIZATION OF SHEAR-SLIP

The specimen with fresh silicone segment interface had considerable shear-slip while the specimen with degraded silicone had virtually none. Fig. 3 (a) shows the shear-slip response at segment joints with fresh silicone when specimen was subjected to lateral force. Shear-slip can be represented by the rigid bilinear load (F)-displacement (U) relationship shown in Fig. 3 (b). The stiffness prior to the initiation of shear-slip is assumed to be infinite. The shear-slip initiates once the lateral force overcomes friction developed at joint interface (F_s). The shear-slip stiffness (k_s) is defined as the slope of the shear force with respect to shear-slip after shear-slip is initiated. The shear-slip force (F_s) is equal to the friction force, and assumed to be the product of normal force and coefficient of friction.

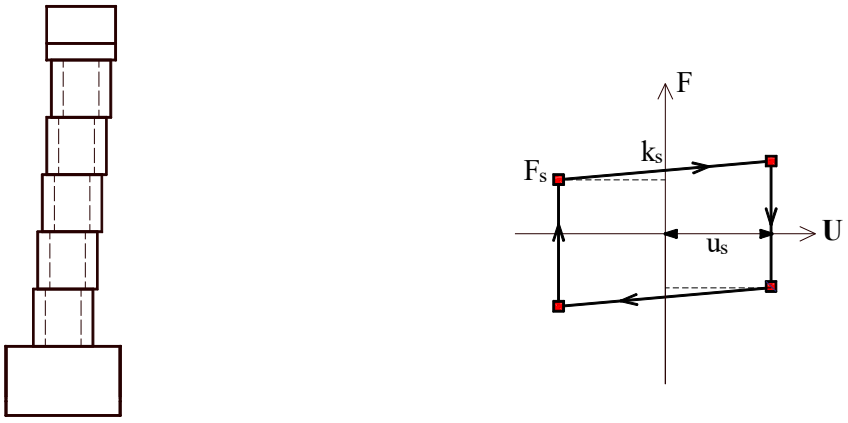

(a) (b)

Fig. 3 (a) Joint shear-slip mechanism, (b) shear-slip hysteretic response

Shear force is plotted against shear-slip for all loading cycles in Fig. 4 (a) as obtained from the test in which shear-slip governed the response. Stiffer response at the end of each cycle is due to rocking. When shear-slip is accompanied by rocking, post-tensioning force increases and leads to a continuous increase of normal force between segments. Post-tension force versus shear-slip is also shown in Fig. 4 (b) given the dependence of friction force on normal axial load. Shear-slip stiffness (k_s) for each cycle was calculated using the data shown in Fig. 4 (a) by linear regression.

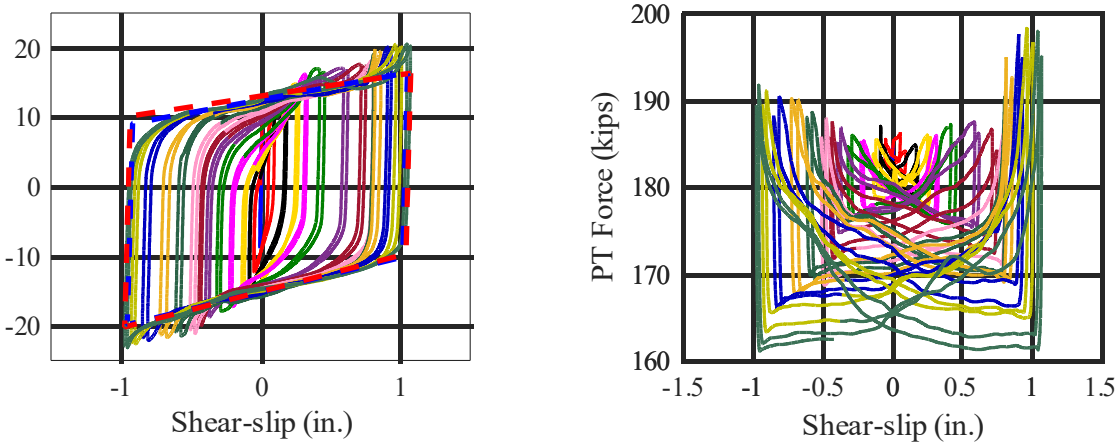

(a) (b)

Fig. 4 (a) Shear force and (b) PT force versus shear-slip

The friction coefficient was then calculated by dividing the shear force by the normal force. The normal force is assumed to be equal to the post-tension force. The component of lateral force perpendicular to the interface due to rocking displacement was small and neglected. The component of the post-tension force in the lateral direction was also small and neglected. Friction coefficient is plotted against shear-slip, as shown in Fig. 5. Two lines were fitted onto Fig. 5 using the least-squares method for each cycle representing shear-slip being locked

and activated. The friction coefficient for each cycle was assumed to be the intersection of these two lines.

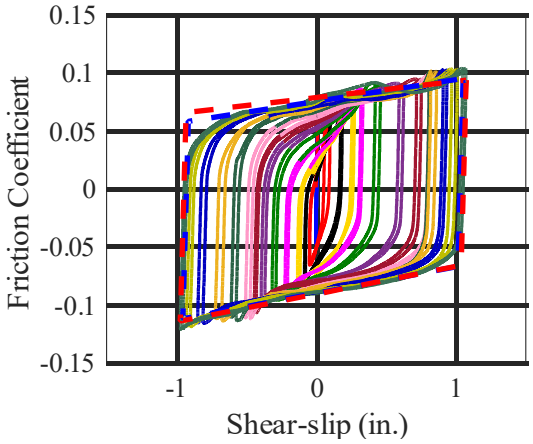

Fig. 5 Friction coefficient versus shear-slip

The friction coefficient and shear-slip stiffness are the two important parameters required to characterize the shear-slip response. The friction coefficient and shear-slip stiffness, as identified by testing, are plotted at different loading cycles in Fig. 6. The calculated friction coefficient and shear-slip stiffness varied up to the 10th cycle. After then, both converged to constant values. The increase of friction coefficient with the increasing number of cycles may be mainly due to multiple and varying number of joints participating in shear-slip, and secondarily due to the variation of normal force, frictional heating, and cumulative movement.

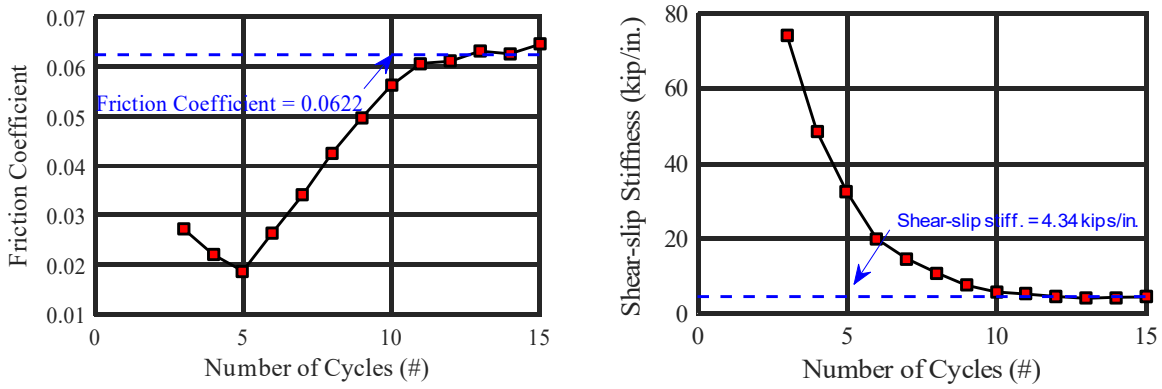

Fig. 6 (a) Friction coefficient and (b) shear-slip stiffness at different loading cycles

The friction coefficient and shear-slip stiffness are taken as the average of the cycles where the shear-slip response become constant (friction coefficient = 0.0622; shear-slip stiffness = 4.34 kips/in.).

ANALYTICAL MODEL AND VALIDATION

An analytical model is established for post-tensioned segmental precast concrete bridge pier for three scenarios: shear-slip being disallowed, shear-slip occurring before rocking starts, and shear-slip occurring after rocking starts. Whether and when the shear-slip occurs depends on the friction coefficient at segment interfaces. All segment interfaces were assumed to have the same properties so that shear-slip initiates at all joints simultaneously.

ANALYTICAL MODEL FOR NO SHEAR-SLIP

Precast segments with shear-keys, or with segment interface materials like degraded silicone, will not undergo shear-slip, and the response will be dominated by rocking. Fig. 7 (a) depicts rocking before and after the gap opening. The analytical model for rocking precast post-tensioned segmental column with unbonded strands was developed by Hewes and Priestley[1] and Pampanin et al.[22] is used herein to establish the lateral force-displacement relationship for the specimens tested.

The behavior is characterized by four key stages of response, as seen in Fig. 7 (b). Stage O-A represents the response prior to decompression at bottom joint. During this stage, the curvature is linearly distributed from the top to the bottom of the column, and moment-area theory is used to calculate the tip displacement. Point A indicates the initiation of partial separation at the tension face. The contact area decreases during stage A-B. After point B, a nonlinear stress distribution will be formed over the contact area in compression to sustain the reaction force. The base curvature increases with the increase of concrete strain at the extreme compression fiber. Gap opening is calculated by assuming that the nonlinear stress zone covers half of the cross section's depth. At stage B-C, post-tensioning strands, especially located eccentrically, were subjected to extension due to gap opening. Post-tensioning force provides the main source of the stiffness at B-C stage. The strength at stage C-D converges to a constant value due to tendon yielding.

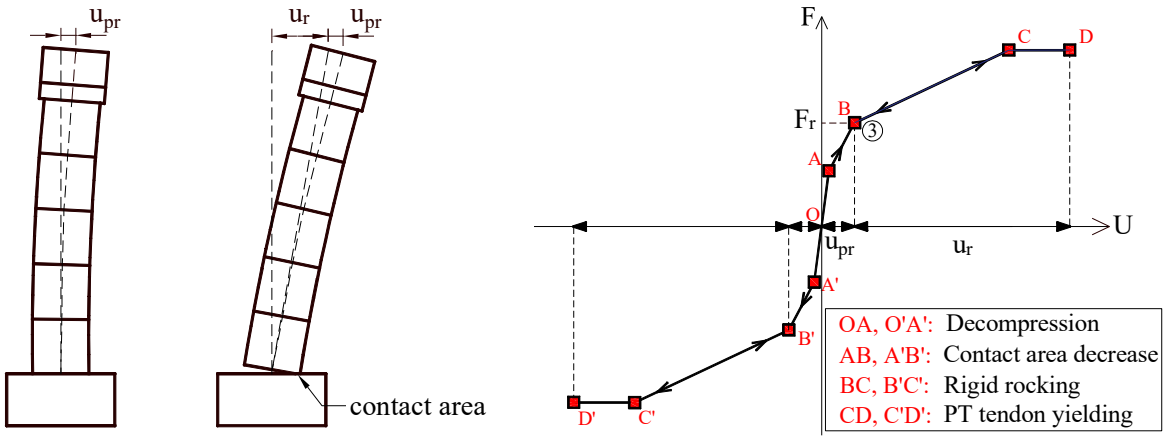

(a) (b)

Fig. 7 (a) Rocking, and (b) analytical model for no shear-slip

ANALYTICAL MODEL FOR WHEN SHEAR-SLIP IS ALLOWED BEFORE ROCKING

If two precast concrete pier segments, with interface material like fresh silicone, have sufficiently high enough friction coefficient, shear-slip can initiate before rocking. Fig. 8 (a) shows the analytical model for rocking only. The post-tensioning tendons are assumed to remain within the elastic range. The hysteretic response is idealized to be a bilinear curve, representing two stages: pre-rocking (decompression and decrease of contact area) and rocking. Three key parameters: pre-rocking stiffness (k_{pr}), rocking force (F_r), and rocking stiffness (k_r) can be calculated. Fig. 8 (b) shows the shear-slip only bilinear model with the key parameters: shear-slip force (F_s), shear-slip stiffness (k_s).

Fig. 8 (c) shows the combined response of both rocking and shear-slip. The displacement response is a combination of rocking and shear-slip. A two-cycle hysteretic behavior is created from zero displacement to a defined target displacement (u_{tgt}). The first and second cycles of the response path are illustrated with the dashed and solid lines, respectively.

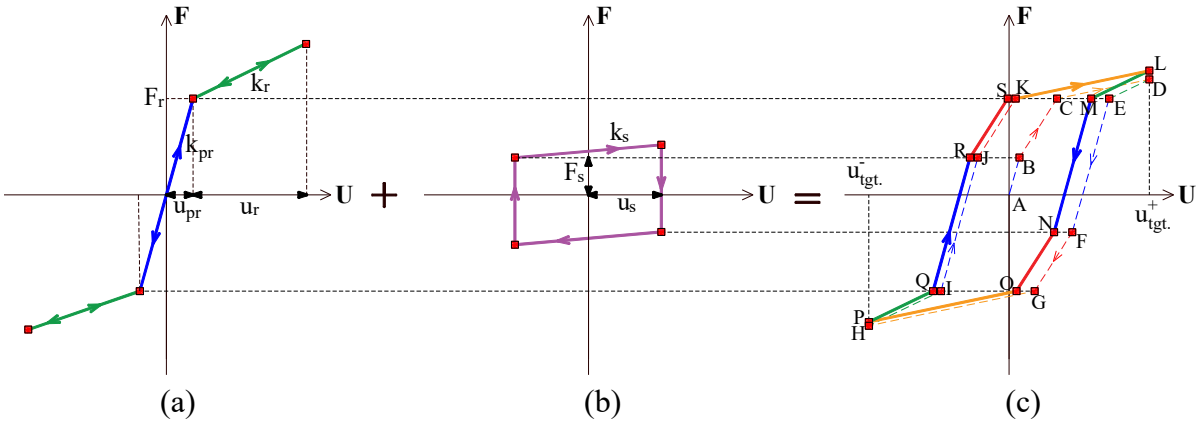

Fig. 8 Hysteretic model for (a) rocking only response, (b) shear-slip only response, and (c) combined response for when shear-slip is allowed before rocking

The formulation of lateral force and displacement relationship under loading and unloading was established based on superposition, as shown in Table 1. Stage A-B corresponds to pure pre-rocking phase. The stiffness of branch A-B is equal to stiffness in the pre-rocking range (k_{pr}). After point B, lateral force reaches the force needed to activate shear-slip (F_s). Stage B-C is subjected to stiffness degradation due to the shear-slip. The response is calculated as a combination of pre-rocking and shear-slip until the rocking force (F_r) is reached. During stage C-D, the rocking force is exceeded and the response is a combination of rocking and shear-slip. Similarly, the stiffness in this stage is less than rocking stiffness (k_r) due to shear-slip.

Once unloading starts, rocking displacement is recovered first. The stiffness of stage D-E is equal to the pre-rocking stiffness (k_r) until the lateral force is reduced to the rocking force (F_r). After that, in stage E-F, pre-rocking displacement is recovered. Pre-rocking and rocking displacements can return to zero upon force removal. Stages of the rest of the first cycle and the second cycle take place in the same order described for stages between A and F. These

stages are grouped according to their behavior in Table 1. In Table 1, X and Y refer to start and end points of a stage, respectively.

Table 1 Analytical formulation for when shear-slip is allowed before rocking

	Stage X-Y	Behavior	Force-displacement relationship	Valid range
Load	A-B, E-F, I-J, M-N, Q-R	Pre-rocking		
	B-C, F-G, J-K, N-O, R-S	Pre-rocking & shear-slip		
	C-D, G-H, K-L, O-P	Rocking & shear-slip		
Un-load	D-E, H-I, L-M, P-Q	Rocking		
	E-F, I-J, M-N, Q-R	Pre-rocking		

ANALYTICAL MODEL FOR WHEN SHEAR-SLIP IS ALLOWED AFTER ROCKING

When the friction coefficient between precast segments is larger, such as in the case of degraded silicone interface material, shear-slip can occur after rocking. Fig. 9 shows the hysteretic response of such a case, as a combination of rocking and shear-slip response. Shear-slip does not start until a later phase, i.e., Regime III. The length of Regime III is determined by the force at which shear-slip occurs. Fig. 9 assumes that shear-slip occurs before the target displacement. When the target displacement is reached at a force not large enough to initiate shear-slip, shear-slip will not contribute to response. This might be the case for segments with high-friction interfaces.

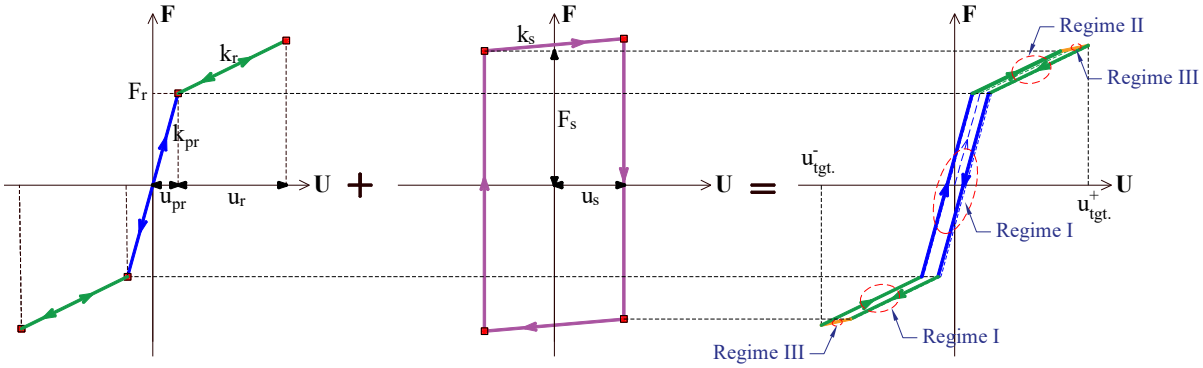

(a) (b) (c)

Fig. 9. Hysteretic model for (a) rocking only response, (b) shear-slip only response, and (c) combined response for when shear-slip is allowed after rocking

Regimes I and II involve pre-rocking and rocking, respectively. Analytical model for these stages are the same as ones for when shear-slip occurs before rocking. The stiffness

decreases in Regime III due to shear-slip. The much narrower hysteresis loop shows the energy dissipation is smaller, and self-centering capability is higher than the one with shear-slip before rocking. The summary of the force-displacement relationship formulations at different regimes is shown in Table 2.

Table 2 Analytical formulation for when shear-slip is allowed after rocking

	Stage	Behavior	Force-displacement relationship	Valid range
Load	Regime I	Pre-rocking	,	
	Regime II	Rocking	,	
	Regime III	Rocking & shear-slip	,	
Un-load	Regime I	Rocking	,	
	Regime II	Pre-rocking	,	

FRICTION COEFFICIENT RANGES

The ranges of friction coefficient (μ) applicable for when no shear-slip occurs, when shear-slip is allowed before rocking, and when shear-slip is allowed after rocking are illustrated in Table 3. The friction coefficient range limits not only depend on the pier's properties (i.e., pre-rocking stiffness k_{pr}, the rocking force F_r and rocking stiffness k_r), the total post-tensioning force (i.e., total normal force: N), but also on the target displacement u_{tgt} under a certain seismic intensity.

Table 3 The range of friction coefficients for different shear-slip conditions

Shear-slip condition	Range of friction coefficient
No Shear-slip	
Shear-slip is allowed before rocking	
Shear-slip is allowed after rocking	

THE INFLUENCE OF SEGMENT INTERFACE CHARACTERISTICS ON SEISMIC RESPONSE

Understanding the response to the variation of interface materials and friction properties can offer opportunities to optimize hysteresis response. Using the analytical model established, the influence of precast segmental friction interface on response is investigated. Segment interface material was varied from fresh silicone to materials often used in other sliding structural systems. These materials are presented in Table 4. Geometry and properties of the precast pier and the initial post-tensioning force were kept constant.

Table 4 Friction coefficients for different interface materials

Nomenclature	Interface Materials	Friction coefficient
Reference	Concrete against concrete with fresh silicone interface	0.06
Material-1	Dimpled lubricated PTFE sheets against stainless steel	0.04[23]
Material-2	Unfilled/Woven PTFE fiber against stainless steel	0.08[23]
Material-3	Leaded-bronze against stainless steel	0.190[20]
Material-4	Leaded-bronze against alloy cast steel	0.161[20]
Material-5	Concrete against dry concrete	0.6[24]

The analytical model developed was used to construct hysteretic loops for pier systems with varying segment interface materials. The hysteretic loops for these different friction interface materials are compared in Fig. 10. The target displacement was set to be 2.75 in. (2.1% lateral drift ratio), which represented the median of peak displacement at DE level obtained through shake-table testing of similar specimens[25]. This target displacement ($u_{tgt.}$) is assumed large enough to initiate rocking. The black solid line is representing the concrete-to-concrete interface with fresh silicone.

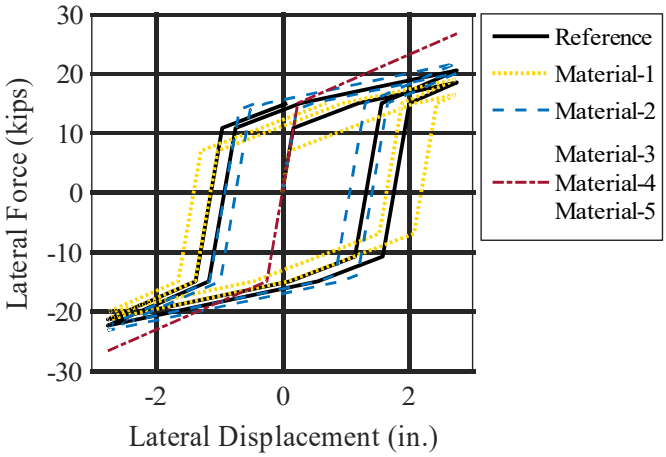

Fig. 10. Comparison of hysteresis loops for different interface materials

The hysteresis loop becomes fatter for materials with lower friction coefficients as expected. For Material-3 to Matterial-5, the hysteresis loops are very narrow, indicating negligible energy dissipation. The loading and unloading is bilinear and virtually overlap. In addition, as the friction between segments decrease, the lateral strength at the target displacement decreases. This confirmed that shear-slip weakens the response.

The equivalent (secant) stiffness, equivalent viscous damping ratios, and residual displacement ratios were calculated for values of friction coefficient from 0.02 to 0.15. The equivalent stiffness can capture the reduction in the lateral stiffness due to various levels of rocking and shear-slip. Natural period of structure and the corresponding seismic force can be evaluated based on this stiffness. Similarly, equivalent viscous damping ratio is an

indicator of energy dissipation capacity. Increasing values indicate higher energy dissipation. Fig. 11 (a), (b), and (c) present the sensitivity of the equivalent stiffness, equivalent viscous damping ratios, and residual displacement ratios to changes in friction coefficient.

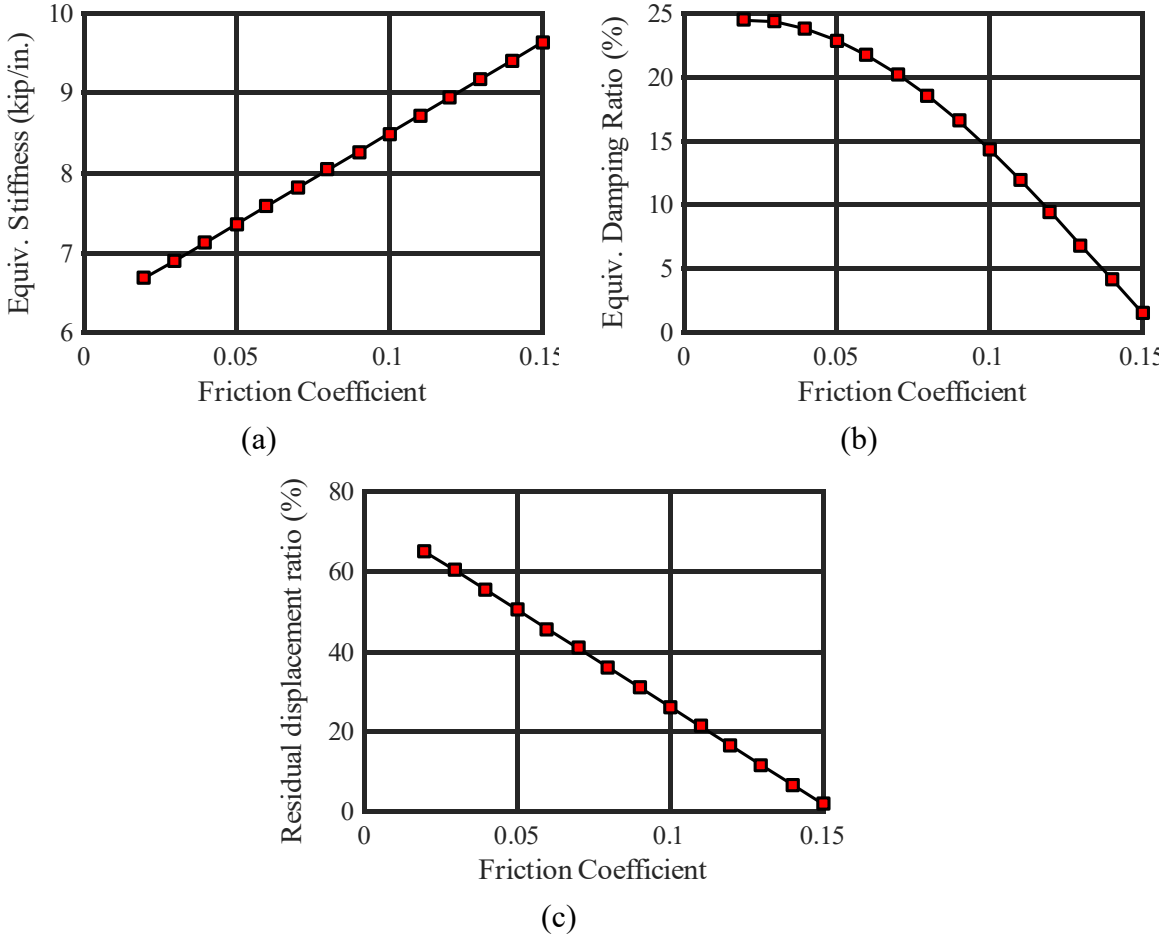

Fig. 11 Relationship of (a) secant stiffness, (b) equivalent damping ratio, and (c) residual displacement ratio with friction coefficient

The results show that increase in friction coefficient causes the equivalent stiffness to increase and the equivalent viscous damping ratio to decrease. Reducing stiffness using a low friction interface material can decrease maximum acceleration and the associated force. Using a low friction material can also increase energy dissipation. It should be noted, however, that shear-slip introduces residual displacements.

SUMMARY AND CONCLUSIONS

This paper presented experimental results of the response of large-scale precast post-tensioned concrete segmental pier specimen with fresh silicone and degraded silicone segment interfaces to quasi-static cyclic lateral loading. Pier specimen had unbonded post-tensioning which allowed self-centering upon removal of the load. Shear-slip response

obtained from test results was used to characterize segment interface frictional properties. An analytical model, which incorporated rocking and shear-slip at varying proportions, was created. The analytical model was used to understand the impact of friction properties of commonly used interface materials on global response. Finally, a parametric study utilizing the analytical model was conducted to report the sensitivity of results to values of friction coefficient. The major contributions and conclusions of this paper are as follows:

Test results showed that the essential difference in the performances of precast pier with fresh silicone and degraded silicone segment interfaces was that the former exhibited greater energy dissipation, at the expense of reduced self-centering capability. Reduced self-centering capability reveals itself through residual displacements or misalignment of segments.

The shear-slip, if any, can be characterized using the rigid bilinear relationship between lateral force and displacement. Key parameters to identify from this relationship were force needed to activate shear-slip, and stiffness before and during shear-slip. Additional research is needed to formulate a relationship between friction coefficient and shear-slip stiffness of a given material, considering the effects of rocking behavior and post-tensioning force change.

An analytical model was established to predict hysteresis response for post-tensioned segmental precast concrete bridge piers. The model can be used as a simple tool for seismic design of precast segmental piers with various interface friction properties. The analytical model was used to investigate the response for piers with a variety of materials used in sliding structural systems. Precast pier seismic response can be improved in two ways by introducing low friction coefficient materials at segmental interface: 1) energy dissipation capability was enhanced; 2) lateral stiffness was decreased, leading to a shift of natural period and decrease in seismic acceleration. However, the greatest disadvantage of allowing shear-slip through low friction segment interface materials is the loss of self-centering capability. Even though damage to concrete is largely reduced, the designer should consider the compromise between energy dissipation and residual displacements when selecting the system.

Most sliding structural systems require maintenance to perform as expected. The results of the analytical model shows that unexpected changes in segment interface conditions and resulting increase in friction coefficient, can significantly change the response. Increasing friction coefficients over the service life due to factors such as aging and environmental changes will limit energy dissipation capacity of the system.

FUTURE WORK

Shear-slip and friction are complex phenomena, which are influenced by multiple factors. Considering the uncertainties in segment surface characteristics and thus shear-slip response, additional work is required to quantify the variation of interface conditions at segment interface over time and under varying environmental conditions (temperature, humidity, etc.).

Additional experimental data can provide engineers with a range of friction coefficients to be used in design. Alternatively, other interface materials designed for low friction, such as Polytetrafluoroethylene (PTFE), can be investigated using similar methods before implementation to address constructability and durability issues.

ACKNOWLEDGMENTS

The authors gratefully acknowledge the financial support provided by Federal Highway Administration (FHWA) through the Multidisciplinary Center for Earthquake Engineering Research (MCEER) of University at Buffalo. The results, conclusions and opinions given in this paper are the ones of the authors and do not necessarily reflect the views of the funding agencies and the parties acknowledged.

REFERENCES

1. Hewes, J. T., and Priestley, M. J. N., "Seismic design and performance of precast concrete segmental bridge columns." Rep. No. SSRP-2001/25, Univ. of California at San Diego, 2002.
2. Mander, J. B., and Cheng, C. T., "Seismic resistance of bridge piers based on damage avoidance design." Technical Rep. NCEER-97-0014, State Univ. of New York, Buffalo, N.Y., 1997.
3. Yang, C. and P. Okumus, "Performance of Ultra-high Performance Concrete Self-centering Bridge Piers under Seismic Loads." *Istanbul Bridge Conference*. Istanbul, Turkey, 2016.
4. Priestley, M., et al., "Preliminary results and conclusions from the PRESSS five-story precast concrete test building." *PCI Journal,* V. 44, No. 6, 1999, pp. 42-67.
5. Lee, W., Jeong, H., Billington, S., Mahin, S. A., and Sakai, J., "Post-tensioned structural concrete bridge piers with self-centering characteristics." *Proc., Structural Congress*, ASCE, Reston, VA, 2007, pp.1-15.
6. Ou, Y., Chiewanichakorn, M., Aref, A. J., and Lee, G., "Seismic performance of segmental precast unbonded posttensioned concrete bridge columns." *Journal of Structural Engineering,* V. 133, No. 11, 2007, pp. 1636-1647.
7. Palermo, A., Pampanin, S., and Marriott, D., "Design, Modeling, and Experimental Response of Seismic Resistant Bridge Piers with Posttensioned Dissipating Connections." *Journal of Structural Engineering,* V. 133, No. 11, 2007, pp. 1648-1661.
8. Chou, C., and Chen, Y., "Cyclic tests of post-tensioned precast CFT segmental bridge columns with un-bonded strands." *Earthquake Engineering & Structural Dynamics,* V. 35, No. 2, 2006, pp. 159-175.
9. ElGawady, M. A., and Sha'lan, A., "Seismic behavior of self-centering precast segmental bridge bents." *Journal of Bridge Engineering,* V. 16, No. 3, 2010, pp. 328-339.

10. Mashal, M. and A. Palermo., "Experimental Testing of Emulative Fully Precast Concrete Bridge Bent in Seismic Regions,", *Australasian Structural Engineering Conference*. 2014. Auckland, New Zealand.
11. Morgen, B.G. and Y.C. Kurama, "Seismic response evaluation of posttensioned precast concrete frames with friction dampers," *Journal of structural engineering*, V. 134, No. 1, 2008, pp. 132-145.
12. Sideris, P., Aref, A. J., and Filiatrault, A., "Quasi-static cyclic testing of a large-scale hybrid sliding-rocking segmental column with slip-dominant joints." *Journal of Bridge Engineering,* V. 19, No. 10, 2014, 1943-5592.
13. Yang, C. and P. Okumus, "Ultra-high performance concrete for post-tensioned segmental precast bridge piers for seismic resilience." *Journal of Structural Engineering*, Under Review.
14. Constantinou MC, Whittaker AS, Kalpakidis Y, Fenz DM, Warn GP, "Performance of seismic isolation hardware under service and seismic loading." *MCEER-07-0012, Multidisciplinary Center for Earthquake Engineering Research*, State University of New York, Buffalo, NY, 2007.
15. Kumar, M., A.S. Whittaker, and M.C. Constantinou, "Characterizing friction in sliding isolation bearings." *Earthquake Engineering & Structural Dynamics,* V. 44, No. 9, 2015 pp. 1409-1425.
16. Hwang, J., K. Chang, and G. Lee, "Quasi-static and dynamic sliding characteristics of Teflon-stainless steel interfaces." *Journal of Structural Engineering,* V. 116, No. 10, 1990, pp. 2747-2762.
17. Mokha, A., M. Constantinou, and A. Reinhorn, "Teflon bearings in base isolation I: Testing." *Journal of Structural Engineering,* V. 16, No. 2, 1990, pp. 438-454.
18. Thompson, J. B., Turrell, G. C. and Sandt B. W., "The Sliding Friction of Teflon." *SPE Journal,* V. 11, No. 4, 1955, pp. 13-14.
19. Campbell, T. I., Pucchio, C. B., Roeder, C. W., and Stanton, J. F., "Frictional characteristics of PTFE used in slide surfaces of bridge bearings." *Proc. 3rd World Conf. on Bearings for Concrete Structures*, American Concrete Institute, 1991, pp. 847-870.
20. Morgen, B.G. and Y.C. Kurama, "Characterization of two friction interfaces for use in seismic damper applications". *Materials and Structures*, 2009. 42(1): pp. 35-49.
21. McVitty, W.J. and M.C. Constantinou, "Property Modification Factors for Seismic Isolators: Design Guidance for Buildings." *MCEER-15-0005, Multidisciplinary Center for Earthquake Engineering Research*, State University of New York, Buffalo, NY, 2015.
22. Pampanin, S., M.J. Nigel Priestley, and S. Sritharan, "Analytical Modelling of the Seismic Behavior of Precast Concrete Frames Designed with Ductile Connections." *Journal of Earthquake Engineering,* V. 5, No. 3, 2001, pp. 329-367.
23. AASHTO. (2011) "Guide Specifications for LRFD Seismic Design." Washington, D.C
24. ACI (American Concrete Institute). (2014), "Building Code Requirements for Structural Concrete and Commentary." *ACI 318- 14 and ACI 318R-14*, Farmington Hills, MI.

25. Sideris, P., Aref, A. J., and Filiatrault, A., "Large-scale seismic testing of a hybrid sliding-rocking posttensioned segmental bridge system." *Journal of Structural Engineering*, V. 140, No. 6, pp. 1943-541X